



HAL
open science

Response to and recovery from nitrogen and silicon starvation in *Thalassiosira weissflogii*: growth rates, nutrient uptake and C, Si and N content per cell

Christina L. de La Rocha, Anja Terbrueggen, Christoph Voelker, Soenke Hohn

► To cite this version:

Christina L. de La Rocha, Anja Terbrueggen, Christoph Voelker, Soenke Hohn. Response to and recovery from nitrogen and silicon starvation in *Thalassiosira weissflogii*: growth rates, nutrient uptake and C, Si and N content per cell. *Marine Ecology Progress Series*, 2010, 412, pp.57-68. 10.3354/meps08701 . hal-00518109

HAL Id: hal-00518109

<https://hal.univ-brest.fr/hal-00518109v1>

Submitted on 19 Dec 2021

HAL is a multi-disciplinary open access archive for the deposit and dissemination of scientific research documents, whether they are published or not. The documents may come from teaching and research institutions in France or abroad, or from public or private research centers.

L'archive ouverte pluridisciplinaire **HAL**, est destinée au dépôt et à la diffusion de documents scientifiques de niveau recherche, publiés ou non, émanant des établissements d'enseignement et de recherche français ou étrangers, des laboratoires publics ou privés.



Distributed under a Creative Commons Attribution 4.0 International License

Response to and recovery from nitrogen and silicon starvation in *Thalassiosira weissflogii*: growth rates, nutrient uptake and C, Si and N content per cell

Christina L. De La Rocha^{1,*}, Anja Terbrüggen², Christoph Völker², Sönke Hohn^{2,3}

¹Laboratoire des Sciences de l'Environnement Marin (LEMAR), Institut Universitaire Européen de la Mer, Université de Bretagne Occidentale, Place Copernic, Technopôle Brest-Iroise, 29280 Plouzané, France

²Alfred-Wegener-Institut für Polar- und Meeresforschung, Am Handelshafen 12, 27570 Bremerhaven, Germany

³GKSS Research Center, Max-Planck-Strasse 1, 21502 Geesthacht, Germany

ABSTRACT: Understanding the response of diatoms to nutrient stress is important, both on its own terms and for the accurate portrayal of this key group of organisms in ecological and biogeochemical models. We therefore examined the growth and elemental composition of *Thalassiosira weissflogii* grown to nutrient depletion and then its recovery after nutrient readdition. During nitrate starvation, *T. weissflogii* continued dividing, producing cells with low quotas of N, P and Si. After nitrate readdition, cells immediately began taking up nitrate at relatively low net cell-specific rates and rebuilding cellular stores of all nutrients. More than 30 h elapsed before there was a visible increase in cell numbers. Cellular C/N and C/P ratios remained high and N/P ratios remained low for the remaining 45 h of the experiment. Cells in the silicon starvation experiment abruptly ceased dividing at 1 to 3 μM dissolved silicon (DSi) and immediately resumed dividing upon the resupply of DSi. Growth rates and net cell-specific rates of silicon uptake recovered to maximal values within 3 to 7 h, but net cell-specific rates of nitrate and phosphate never did, causing a decline in N and P content per cell during the whole experiment. Ratios of C/N and N/P remained close to Redfield values. While cell-specific rates of silicon uptake correlated strongly with DSi concentrations during all portions of the silicon starvation experiment, they were directly related to cellular growth rates during the nitrogen starvation experiment, suggesting that during nitrate starvation silicon acquisition was acting as the rate-limiting step for cell division.

KEY WORDS: *Thalassiosira weissflogii* · Nitrogen starvation · Silicon starvation · C/N · Si per cell

Resale or republication not permitted without written consent of the publisher

INTRODUCTION

Phytoplankton growing in highly productive upwelling systems must frequently respond to a pulse of nutrients after a period of nutrient limitation or starvation. Bloom-forming diatoms appear to be adept at this, and species such as *Thalassiosira weissflogii* tend to dominate the initial blooming after such nutrient input (Smetacek 1985).

Unlike virtually all other major bloom-forming phytoplankton, diatoms require silicon as a major

nutrient and can therefore be limited by low to negligible concentrations of dissolved silicon (DSi). This can occur at times when other phytoplankton either are not nutrient limited or are limited instead by low concentrations of nitrogen or phosphorus. Diatoms may even push their localities into silicon limitation through the 'silicate pump', in which biogenic silica sinks to deeper depths than does particulate organic matter before remineralization (Dugdale et al. 1995). For example, judging from the eWOCE data set (Schlitzer 2000), DSi to nitrate ratios above 600 m depth in the ocean are, on

*Email: christina.delarocha@univ-brest.fr

average, less than 1 mol mol^{-1} (De La Rocha 2007). This is less than the typical utilization ratio of 1 mol mol^{-1} of nutrient-replete diatoms (Brzezinski 1985), while the ratio in the deep sea ($\sim 3 \text{ mol mol}^{-1}$) is well in excess. Given that not all phytoplankton are diatoms means that a DSi to nitrate ratio in upwelling waters lower than the typical diatom Si:N utilization ratio does not necessarily result in silicon limitation of diatoms. However, it is tempting to wonder whether the excess removal of Si from the surface ocean is just an unfortunate trade-off for the protective (or other) advantages of the siliceous frustule, or if silicon limitation is somehow advantageous to diatoms. For example, diatoms appear to recover more quickly from silicon starvation than from nitrogen starvation and this might help them compete for newly upwelled nutrients (De La Rocha & Passow 2004).

There is much literature on diatom physiology that portrays a general picture of the response of diatoms to nutrient limitation and starvation. Diatom cells moving into silicon limitation and then starvation may become more thinly silicified, but at the same time they may contain ample supplies of N and build up increased stores of P and C (Coombs et al. 1967, Harrison et al. 1976, 1977, 1990, Flynn & Martin-Jézéquel 2000, Martin-Jézéquel et al. 2000, De La Rocha & Passow 2004). However, nitrogen-limited or nitrogen-starved cells are likely to be nitrogen poor and deficient in enzymes and proteins, such as nitrate reductase and chlorophyll (Harrison et al. 1976, 1977, Sakshaug & Holm-Hansen 1977, Dortch 1982), that would need to be synthesized before cell growth could resume at normal rates.

The present study aimed to investigate the parallel responses of a bloom-forming diatom to nitrate and DSi starvation and to record the attendant changes in the elemental composition and nutrient uptake rates of the cells. We grew *Thalassiosira weissflogii* to a brief period of nitrate- or DSi-starvation and tracked its recovery following readdition of the missing nutrient. In so doing, we have also produced a data set that we hope will complement previous studies (e.g. Laws & Bannister 1980, Flynn et al. 1994) in its usefulness to the development and testing of models of phytoplankton physiology.

METHODS

Cultures of the marine diatom *Thalassiosira weissflogii* were kept in exponential growth phase in artificial seawater (Ulramarine Synthetica, Waterlife Research) on a 16 h light:8 h dark cycle at 15°C for several weeks before the start of the experiments. These pre-experimental cultures were grown in *f/2* media (Guillard 1975) except that the initial nitrate concen-

tration in the media of cells to be used in the nitrogen starvation experiment and the initial dissolved silicon (DSi) concentration in the media of cells to be used in the silicon starvation experiment were one-half that normally contained in *f/2* media.

Nitrogen starvation experiment. Exponential phase *Thalassiosira weissflogii* cells were inoculated into a growth medium with initial nutrient concentrations of $35 \mu\text{M}$ nitrate, $13 \mu\text{M}$ phosphate and $104 \mu\text{M}$ DSi. The cells were allowed to grow until they had removed all the nitrate from the growth medium and then ceased dividing (Fig. 1). Approximately 70 h later, nitrate was added back to the bottles, bringing nitrate concentrations up to $46 \mu\text{M}$ (concentrations of phosphate and DSi were still relatively high, Fig. 2). The recovery of the cells from nitrogen starvation was monitored with particular focus on the first 24 h after nitrate resupply.

Due to the difficulty of working with and repeatedly sampling from a single large volume culture, the nitrogen starvation experiment (NSE), as well as the silicon starvation experiment (SSE) described below, was carried out in eighteen 2 l cultures simultaneously. The reported data are based on analyses from a shifting subset of 2 bottles. The standard deviations of the analyses from 2 bottles are shown as error bars in the figures.

Cell counts were taken throughout the experiment and measured immediately with a Coulter counter. Samples for determination of particulate organic car-

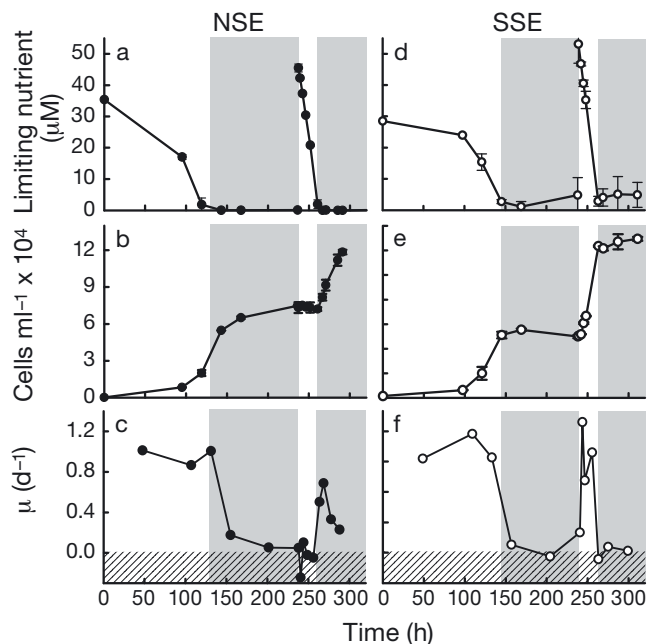


Fig. 1. *Thalassiosira weissflogii*. (a) Nitrate concentrations, (b) cell abundances and (c) growth rates in the nitrogen starvation experiment (NSE), and (d) dissolved silicon concentrations, (e) cell abundances and (f) growth rates in the silicon starvation experiment (SSE). The shaded areas in panels signify the 2 periods when the nutrient was at concentrations low enough to be limiting. Hatched areas contain values below 0

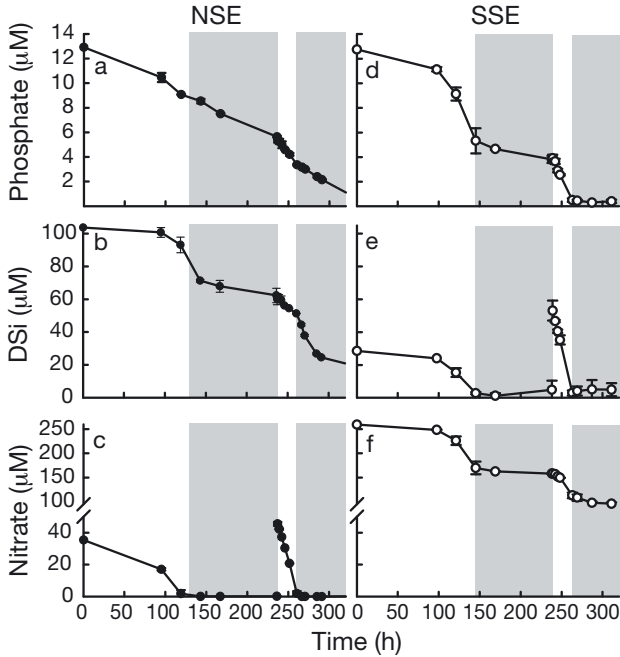


Fig. 2. *Thalassiosira weissflogii*. Nutrient concentrations during the (a–c) NSE and (d–f) SSE experiments; shading as in Fig. 1

bon (POC) and particulate organic nitrogen (PON) concentrations on an elemental analyser (ANCA SL 20-20) were filtered through precombusted GFF filters. Concentrations of nitrate, phosphate and DSi in the filtrate were measured with an autoanalyser (Technicon ASM II). Samples for biogenic silica (BSi) measurements were collected on 0.6 µm polycarbonate filters (Poretics), dried at 60°C, dissolved in 2.5 M HF and analysed for their Si content manually via molybdate blue spectrophotometry (Strickland & Parsons 1972).

The changes in concentrations of nitrate, phosphate and DSi over time were used to roughly estimate rates of nutrient uptake per cell. These specific rates (ρ), in units of moles of nutrient per cell per time, were calculated as:

$$\rho = \frac{C_2 - C_1}{(t_2 - t_1)A_{\text{avg}}} \quad (1)$$

where C_1 and C_2 are concentrations of the nutrient at times t_1 and t_2 and A_{avg} is the average number of cells

per litre in the culture between times t_1 and t_2 . These estimates should not be taken as exact or equivalent to direct measurements of instantaneous rates of nutrient uptake.

Although it was not measured directly, P per cell could be estimated from the decline in phosphate concentrations in the growth media over time (t) and from the increase in cell abundances:

$$P \text{ cell}^{-1} = \frac{[\text{PO}_4]_0 - [\text{PO}_4]_t}{A_t - A_0} \quad (2)$$

where $[\text{PO}_4]_0$ and $[\text{PO}_4]_t$ and A_0 and A_t are the phosphate concentrations and cells per litre at the beginning of the experiment and at time t , respectively.

Silicon starvation experiment. The SSE was carried out exactly as the NSE except that the initial nutrient concentrations were 259 µM nitrate, 13 µM phosphate and 29 µM DSi. *Thalassiosira weissflogii* cells were allowed to grow until the net removal of DSi from the growth medium ceased and the cells stopped dividing (Fig. 1). After 72 h, DSi was added back to the bottles, bringing the DSi concentration up to 53 µM. At this time, concentrations of phosphate and nitrate were still relatively high (Fig. 2). The recovery of the cells to silicon limitation was monitored as described for the NSE.

RESULTS

All directly measured values, such as nutrient concentrations, cell counts and C content per cell, are available (e.g. for modelling) in Tables A1 & A2 in Appendix 1. All elemental data and elemental ratios reported are given in terms of moles and molar ratios.

The experiments were split into 4 different stages based on cell growth and nutrient availability: (1) Initial Growth, (2) 1st Starvation, (3) Recovery and (4) 2nd Starvation (Fig. 1, Table 1). The Initial Growth Stage (IGS) comprised the first ~140 h of the experiment during which nitrate concentrations in the NSE and DSi concentrations in the SSE were drawn down by *Thalassiosira weissflogii* to concentrations that limited diatom growth. In the subsequent 1st Starvation Stage (1st NSS or 1st SSS), concentrations of the limiting nutrient remained low to negligible and cell growth was similarly low to negligible. The readdition of the limiting nutrient around Hour 237 marked the beginning of the Recovery Stage (RS). Because the cultures contained about 6×10^4 cells ml^{-1} at this point, the added nutrient was quickly consumed, leading to the onset of a 2nd Starvation Stage (2nd NSS or 2nd SSS) around Hour 264. During the 2nd SSS,

Table 1. Stages of the experiments

Stage	Nitrogen starvation experiment (NSE)	Silicon starvation experiment (SSE)
Initial Growth (IGS)	0 to 130 h	0 to 145 h
1st Starvation (1st NSS or 1st SSS)	130 to 236 h	145 to 238 h
Recovery (RS)	237 to 261 h	239 to 263 h
2nd Starvation (2nd NSS or 2nd SSS)	261 h to end	263 h to end

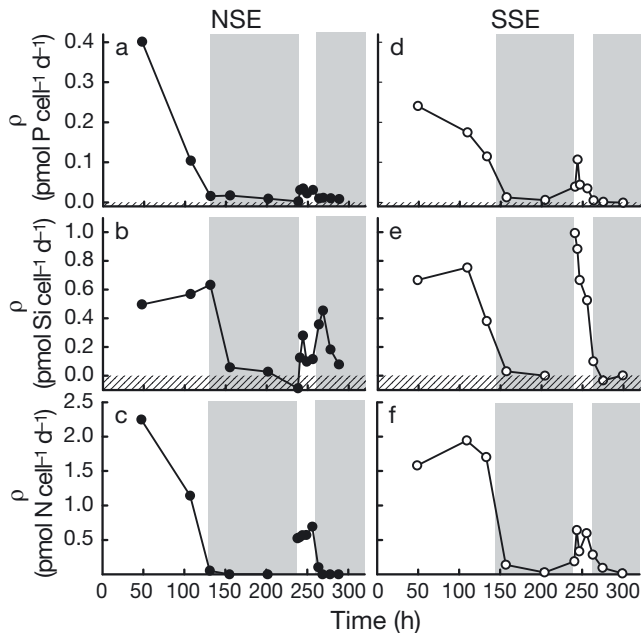


Fig. 3. *Thalassiosira weissflogii*. Specific rates of uptake (ρ) of phosphate, dissolved silicon and nitrate in the (a–c) NSE and (d–f) SSE. Shaded and hatched areas as in Fig. 1

not only were DSi concentrations limiting, but phosphate concentrations were close to exhaustion as well (Fig. 2d).

Nitrogen starvation experiment

Initial Growth Stage

As the initial 35 μM nitrate was removed from the cultures by cells growing exponentially at rates around

1 d^{-1} (Fig. 1a–c), phosphate and DSi concentrations also decreased, but remained high enough not to be limiting (Fig. 2a,b). Specific net rates of uptake of nitrate and phosphate declined sharply as nitrate concentrations diminished, but specific net rates of DSi uptake increased slightly (Fig. 3a–c, Table 2). C, N and P content per cell decreased by 20 to 30% in the later hours of the IGS but cellular Si decreased throughout the IGS (and continued to decline through the end of the 1st NSS) (Fig. 4a–d). Cellular C/N ratios remained steady and low at $5.2 \pm 0.3 \text{ mol mol}^{-1}$ (mean \pm SD) (Fig. 5c) while cellular N/P remained steady at $10.3 \pm 0.3 \text{ mol mol}^{-1}$ (Fig. 6a). Cellular Si/N, Si/C, Si/P and C/P ratios, in contrast, increased at the end of the IGS (Figs. 5a,b & 6b,c).

1st Nitrate Starvation Stage

Nitrate was depleted from the cultures sometime between Hours 120 and 140 and although growth rates immediately declined, it took them another 50 to 100 h to approach 0 (Fig. 1a–c). Depletion of phosphate and DSi concentrations continued, albeit at significantly depressed rates (Fig. 3a,b, Table 2). Both Si and N per cell decreased through the 1st NSS, although the difference between samples at 143 and 236 h was significant only for N (t -test: $t = 3.43$, $p = 0.01$, $n = 4$). Values of C and P per cell increased (t -test: $t = -18.80$ for C and -5.16 for P, $p = 0.02$ and $n = 4$ for both elements) (Fig. 4a–d). Cellular C/P, Si/N and C/N ratios rose over this interval (Figs. 5 & 6) due to the steep drop in N per cell and the rise in C per cell. Both Si/P and Si/C ratios decreased after a brief initial increase (Fig. 6b,c) and cellular N/P significantly decreased (Fig. 6a).

Table 2. *Thalassiosira weissflogii*. Nutrient uptake during the nitrogen starvation experiment. See Table 1 for stage abbreviations

Interval (h)	Stage	μ (d^{-1})	Divisions (d^{-1})	Net ρ nitrate ($\text{pmol cell}^{-1} \text{d}^{-1}$)	Nitrate per doubling ($\text{pmol cell}^{-1} \text{d}^{-1}$)	Net ρ DSi (pmol cell^{-1})	DSi per doubling (pmol cell^{-1})	Net ρ phosphate ($\text{pmol cell}^{-1} \text{d}^{-1}$)	Phosphate per doubling (pmol cell^{-1})
0–95	IGS	1.0	1.5	2.2	1.5	0.5	0.3	0.4	0.3
95–119	IGS	0.9	1.3	1.1	0.9	0.6	0.5	0.1	0.08
119–143	NSS	1.0	1.5	0.1	0.03	0.6	0.4	0.02	0.01
143–167	NSS	0.2	0.3	0	0	0.06	0.2	0.02	0.08
167–236	NSS	0.1	0.1	0	0	0.03	0.4	0.009	0.1
237–239	RS	0.1	0.1	0.5	7.1	-0.09	-1.2	0.002	0.03
239–242	RS	-0.2	0	0.5	-	0.1	-	0.03	-
242–246	RS	0.1	0.1	0.6	4.3	0.3	1.9	0.03	0.2
246–252	RS	0	0	0.6	-	0.1	-	0.02	-
252–261	RS	0	0	0.7	-	0.1	-	0.03	-
261–267	NSS	0.5	0.7	0.1	0.1	0.4	0.5	0.01	0.01
267–271	NSS	0.7	1.0	0	0	0.5	0.5	0.01	0.01
271–285	NSS	0.3	0.5	0	0	0.2	0.4	0.01	0.02
285–291	NSS	0.2	0.3	0	0	0.08	0.2	0.008	0.06

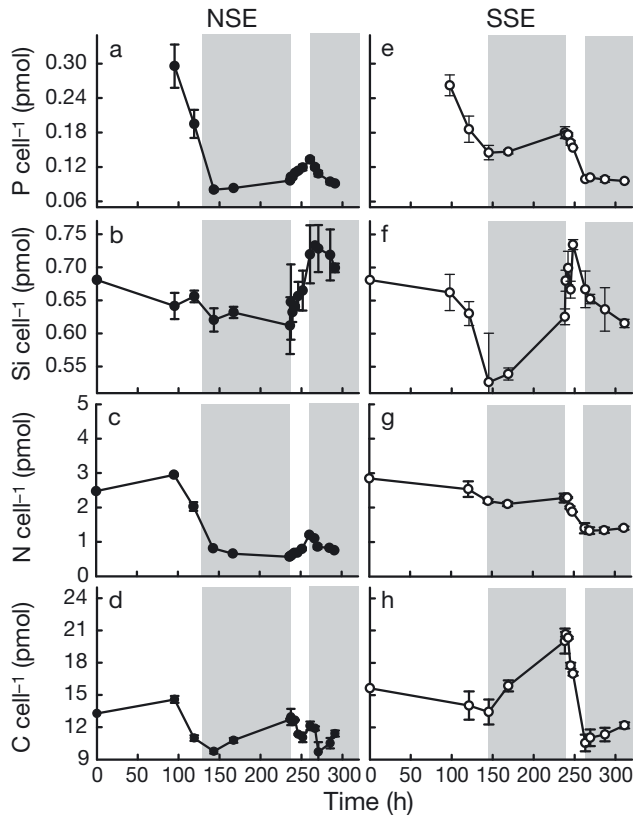


Fig. 4. *Thalassiosira weissflogii*. Quantities of phosphorus, silicon, nitrogen and carbon per cell during the (a–d) NSE and (e–h) SSE. Shading as in Fig. 1

Recovery Stage

Cells did not immediately divide upon the addition of 50 μM nitrate to the nitrogen-starved cultures at Hour 237 (Fig. 1a–c), although they immediately began taking up the added nitrate at a specific net rate of 0.50 pmol nitrate cell⁻¹ d⁻¹ (Fig. 3c). Net uptake of phosphate and DSi also immediately resumed, also at rates that were modest compared with those at the beginning of the experiment (Fig. 3a,b). P, N and Si per cell therefore began to increase because cells were not yet dividing (Fig. 4a–c). C per cell, however, decreased with a 24 h cyclicity, suggesting a net consumption of energy by these recovering cells even during daylight hours (Fig. 4d). These changes in cellular quotas were reflected as drops in cellular Si/N, C/N, Si/P and C/P ratios and increases in Si/C and N/P ratios (Figs. 5a–c & 6a–c).

2nd Nitrate Starvation Stage

Just as the cells had started to divide again, the added nitrate was exhausted from the cultures and the

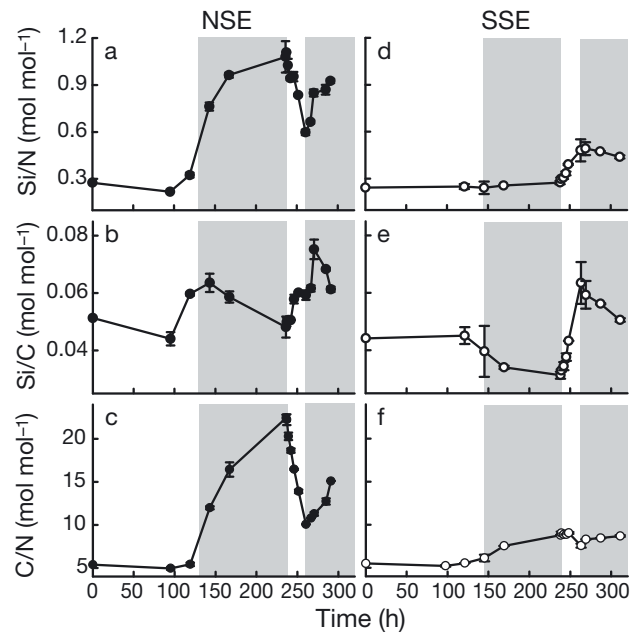


Fig. 5. *Thalassiosira weissflogii*. Cellular Si/N, Si/C and C/N ratios in the (a–c) NSE and (d–f) SSE. Shading as in Fig. 1

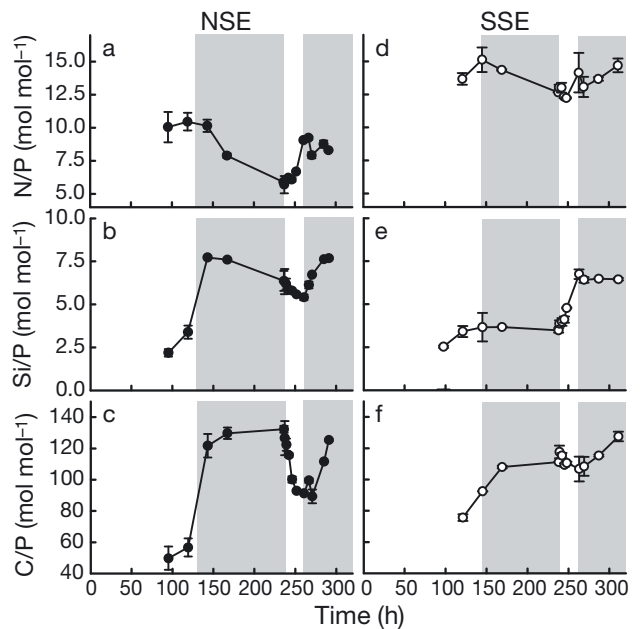


Fig. 6. *Thalassiosira weissflogii*. Cellular N/P, Si/P and C/P ratios in the (a–c) NSE and (d–f) SSE. Shading as in Fig. 1

recovering growth rates began to decline once again (Fig. 1a–c). Net rates of nitrate uptake per cell returned to 0 and those for phosphate and DSi also began to decline (Fig. 3a–c). As a result, P, Si and N per cell all began to decrease (Fig. 4a–c). C per cell, although exhibiting a 24 h cyclicity, showed an overall decline (Fig. 4d). Tracking these changes, cellular Si/N, Si/P,

C/N and C/P rose and cellular Si/C and N/P began to decline (Figs. 5a–c & 6a–c).

Silicon starvation experiment

Initial Growth Stage

During the initial draw down of DSi, *Thalassiosira weissflogii* cells grew exponentially at rates around 1 d^{-1} (Fig. 1d–f). Specific net rates of DSi and phosphate uptake decreased, while those of nitrate uptake remained high (Fig. 3d–f, Table 3). N, C, P and Si per cell all decreased, and the latter two did so dramatically (Fig. 4e–h). The cellular Si/N ratio remained slightly below 0.3 mol mol^{-1} throughout the IGS (Fig. 5d). The cellular Si/C ratio began to decrease and cellular C/N ratio increased towards the end of the IGS. Cellular N/P, Si/P and C/P ratios likewise all increased (Fig. 6d–f).

1st Silicon Starvation Stage

By ~145 h, DSi had been depleted to 1 to $3 \mu\text{M}$ (Fig. 1d) and *Thalassiosira weissflogii* abruptly ceased growing (Fig. 1f). Removal of nitrate and phosphate continued, but at severely diminished rates (Figs. 2 & 3). Net DSi uptake ceased and DSi concentrations rose, presumably from the dissolution of some of the $5.5 \times 10^4 \text{ cells ml}^{-1}$ (equivalent to $3.0 \mu\text{mol l}^{-1}$ BSi) that disappeared between Hours 169 and 238. N content per cell barely increased over this interval (Fig. 4g), but increases in C and P per cell were apparent (Fig. 4e,h). The apparent rise in Si content per cell (Fig. 4f), unsupported by rates of DSi removal (Table 3), was probably an artefact of silica debris from dead cells in the

cultures. The increase in C per cell manifested itself as a drop in the cellular Si/C ratio and as a rise in cellular C/N and C/P ratios (Figs. 5e,f & 6f). There was also a drop in the cellular N/P ratio from 15.1 ± 0.9 to $12.7 \pm 0.01 \text{ mol mol}^{-1}$ (Fig. 6d).

Recovery Stage

An increase in diatom cell numbers was visible within 3 h of the readdition of DSi to the silicon-starved cultures (Fig. 1). Between 3 to 6 h after DSi resupply, growth rates recovered to a value (1.3 d^{-1}) similar to those in the early hours of the experiment (1 d^{-1}). Specific rates of nitrate uptake increased from 1st SSS lows to rates only 30% of those before DSi exhaustion (Fig. 3f). This, in combination with the high growth rates, resulted in a 40% drop in N per cell by 30 h after DSi readdition (Fig. 4e). P and C per cell also dropped to minimum values of $0.10 \pm 0.00 \text{ pmol P cell}^{-1}$ and $10.6 \pm 0.8 \text{ pmol C cell}^{-1}$ (Fig. 4e,h). Si content per cell, however, increased, peaking at $0.73 \pm 0.01 \text{ pmol Si cell}^{-1}$ midway through the RS (Fig. 4d). These shifts drove the marked rises in cellular Si/N, Si/C and Si/P ratios (Figs. 5d,e & 6e). Cellular C/N and C/P decreased and N/P rose, but all 3 only did so towards the end of the RS (Figs. 5f & 6d,f).

2nd Silicon Starvation Stage

DSi (and possibly also P) became limiting around Hour 263 (Fig. 2d,e), resulting in a second cessation of growth (Fig. 1f), a cessation in net DSi uptake, a severe decrease in specific rates of phosphate and nitrate uptake (Fig. 3d–f) and a leveling off of cellular N at around $1.3 \text{ pmol N cell}^{-1}$ and of cellular P at around

Table 3. *Thalassiosira weissflogii*. Nutrient uptake during the silicon starvation experiment. See Table 1 for stage abbreviations

Interval (h)	Stage	μ (d^{-1})	Divisions (d^{-1})	Net ρ nitrate ($\text{pmol cell}^{-1} \text{ d}^{-1}$)	Nitrate per doubling ($\text{pmol cell}^{-1} \text{ d}^{-1}$)	Net ρ DSi (pmol cell^{-1})	DSi per doubling (pmol cell^{-1})	Net ρ phosphate ($\text{pmol cell}^{-1} \text{ d}^{-1}$)	Phosphate per doubling (pmol cell^{-1})
0–98	IGS	0.9	1.4	1.6	1.2	0.7	0.5	0.2	0.1
98–121	IGS	1.2	1.7	1.9	1.1	0.8	0.4	0.2	0.1
121–145	IGS	0.9	1.4	1.7	1.3	0.4	0.3	0.1	0.07
145–169	SSS	0.1	0.1	0.1	0.8	0.03	0.3	0.01	0.08
169–238	SSS	0	0	0.03	–	0	–	0.006	–
239–242	RS	0.2	0.3	0.2	0.7	1.0	3.4	0.04	0.1
242–245	RS	1.3	1.9	0.6	0.3	0.9	0.5	0.1	0.05
245–248	RS	0.7	1.0	0.3	0.3	0.7	0.7	0.04	0.04
248–263	RS	1.0	1.4	0.6	0.4	0.5	0.4	0.03	0.02
263–269	SSS	–0.1	0	0.3	–	0.1	–	0.005	–
269–287	SSS	0.1	0.1	0.09	1.0	0	0	0.001	0.01
287–311	SSS	0	0	0.01	–	0	–	0	–

0.10 pmol P cell⁻¹ (Fig. 4e,g). C content per cell began to increase from the minimum that had been attained at Hour 263. The Si content of cells continued to decline (Fig. 4d) and, as a result, cellular Si/N, Si/C and Si/P ratios also declined (Figs. 5d,e & 6e). Cellular C/N, N/P and C/P ratios increased slightly through the end of the experiment (Figs. 5f & 6d,f).

DISCUSSION

Cell growth during nutrient starvation and recovery

Thalassiosira weissflogii cells kept dividing for 50 to 100 h after the exhaustion of nitrate from their growth medium in the NSE. Such continued division of the cells means that cellular stores of nitrogen became spread out over several divisions' worth of daughter cells, driving a decline in the amount of N per cell to 20 to 80% of nutrient-replete values (Fig. 4b; Harrison et al. 1977, Dortch 1982, Dortch et al. 1984, Harrison et al. 1990, De La Rocha & Passow 2004). During this decline, N would have been shifted out of nonessential pools and into ones critical for the survival of the cell (Dortch 1982). First, unassimilated nitrogen in internal pools would have become assimilated. As nitrogen deficiency became more severe, the amount of amino acids and proteins in the cells would have decreased (Dortch 1982, Olson et al. 1986). The cellular C/N ratios in considerable excess of 12 mol mol⁻¹ observed during the 1st NSS and the RS of the NSE can be taken to indicate that protein had dropped to less than 25% of the cellular mass (Geider & La Roche 2002). Much of the decline in protein would have come from losses of chlorophyll and the carbon-fixing enzyme, Rubisco, which would impinge upon the cells' ability to gather energy through photosynthesis (Dortch et al. 1984). What would have been left after the prolonged period of nitrogen starvation were cells that needed to both acquire and assimilate nitrogen before they could divide again and that needed to produce more chlorophyll and Rubisco to re-attain maximal rates of carbon fixation.

The ~30 h lag between the resupply of nitrate to nitrogen-starved cultures and the resumption of cell division (Fig. 1, Table 2) (Collos 1980, Dortch et al. 1984, Vaulot et al. 1987, De La Rocha & Passow 2004) may be partly attributed to the need of the nitrogen-starved cells to take up and assimilate nitrogen. Supporting this view is the doubling of cellular N during the RS, an increase whose significant cost to cellular energy stores is demonstrated by the decline in C content per cell (Fig. 4d) and the precipitous drop in the C/N ratio (Fig. 5c) that occurred at the same time. Also contributing to the lag is that nitrate reductase, an enzyme produced in response to exposure to nitrate

(Dortch et al. 1984), would need to be synthesized after the 70 h period the cells spent in a nitrate-exhausted medium. The recovery of these cells from nitrogen starvation was additionally not helped by cell-specific rates of nitrate uptake whose peak values after nitrogen starvation were 30% of what they had been capable of at the beginning of the experiment (Fig. 7c).

Adding to the delay in cell division would have been the arrest of the nitrogen-starved cells early in the G1 phase of the cell cycle (Vaulot et al. 1987). (The cell cycle consists of G1, S, G2 and M phases. Nutrient uptake generally occurs during G1 and/or G2 [Vaulot et al. 1987, Brzezinski et al. 1990, Brzezinski 1992], DNA is replicated during the S phase and cell division [mitosis] occurs during M.) Even under the optimal conditions of exponential phase growth, it would have taken at least 8 h for the nitrogen-starved cells of *Thalassiosira weissflogii* to complete the cell cycle from G1 and divide (Vaulot et al. 1987). Cells starved of Si, however, frequently arrest in G2, immediately before mitosis and cell division (Brzezinski et al. 1990). That this occurred in these experiments is suggested by the highest cellular quotas of C in both experiments occurring at the end of the 1st SSS (Fig. 4)

It is unlikely that the need to acquire P or Si added to the delay in cell division. During the RS, cellular N increased by 110% (0.6 pmol N cell⁻¹) to values that

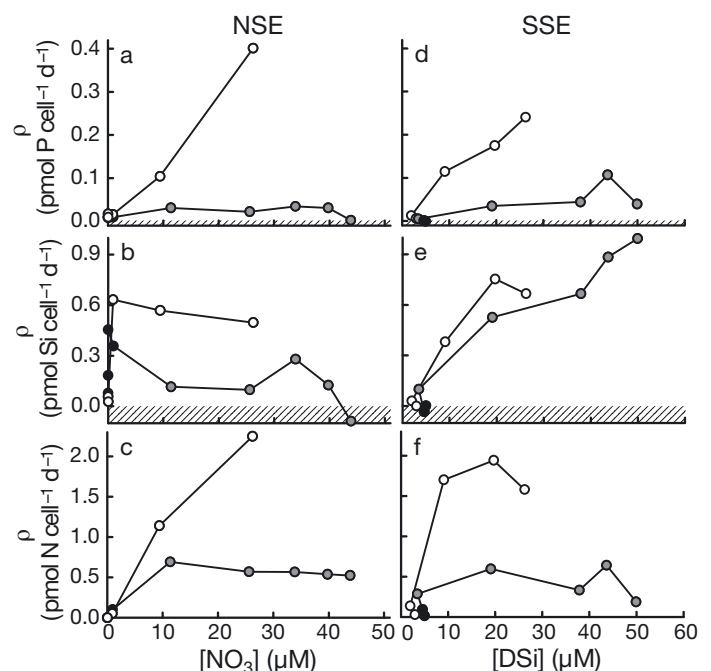


Fig. 7. *Thalassiosira weissflogii*. Cell-specific rates of net phosphate, DSi and nitrate uptake versus the concentration of the limiting nutrient in the (a–c) NSE and (d–f) SSE. Hatched areas contain values below 0. (○) IGS and 1st Starvation Stage, (◐) Recovery Stage, (●) 2nd Starvation Stage

were still lower than those of cells in the nutrient-replete IGS (Fig. 4c). Over this same interval, P content per cell increased by only 40% ($0.04 \text{ pmol cell}^{-1}$) (Fig. 4a) and for most of the RS, the cellular N/P ratio remained below 7 mol mol^{-1} , roughly half of the expected nutrient-replete value of 15 mol mol^{-1} (Fig. 6a). Likewise, Si per cell only increased by 20% ($0.12 \text{ pmol cell}^{-1}$) and that increase was to values in excess of those seen during the IGS (Fig. 4b). Furthermore, the cellular Si/N ratio remained above 0.6 mol mol^{-1} , a value significantly higher than the 0.3 mol mol^{-1} of the nutrient-replete growth early in the experiment (Fig. 5a).

The lower rates of phosphate and DSi uptake relative to rates during the IGS (Fig. 7a,b) may reflect the poor physiological state of the nitrogen-starved cells; not only are the cells' quotas of P and Si (and N) low, but also the cells appear not to have maintained their full set of uptake systems for phosphate and DSi. While it could be argued that the loss of nitrate uptake capacity was due to the growth of the cells for a few days in nitrate-free media (Dortch et al. 1984), the high concentrations of DSi and phosphate in the media make it easier to link the loss of DSi and phosphate uptake capacity to the general loss of proteins from nitrogen-starved cells (since the uptake systems are proteins, Martin-Jézéquel et al. 2000).

In contrast to the nitrogen-starved cells, the diatoms immediately ceased dividing when they came close to exhausting DSi from their growth medium. This put the silicon-starved cells in a completely different situation from the nitrogen-starved cells. No change in the amount of N per cell was observed during the period of silicon starvation (Fig. 4e; also Harrison et al. 1976, 1977), making these cells likely to have been in possession of their full complement of amino acids and proteins (barring those synthesized during the biomineralization of the cell wall, Blank et al. 1986). In addition, some portion of the silicon-starved cells of *Thalassiosira weissflogii* would have arrested in the G2 phase of the cell cycle and would have been able to divide immediately upon the resupply of DSi (Vaulot et al. 1987). This would help to explain the resumption of growth in the SSE so soon after DSi readdition (Fig. 1).

Physiological state at the end of the recovery stage

Cellular ratios of C, N and P (Fig. 6) suggest that at the end of the RS (24 h after nutrient readdition), cells in the SSE were more physiologically 'normal' than were cells in the NSE. Elemental ratios at this point in the SSE were close to typical nutrient-replete values (cellular N/P ratio was 14 mol mol^{-1} and cellular C/N ratio was 7.6 mol mol^{-1}). In the NSE, however, the cel-

lular N/P ratio was only 9 mol mol^{-1} despite increasing by 3.4 mol mol^{-1} during the 24 h of recovery. The cellular C/N ratio, despite dropping by 55% due to nitrate uptake and consumption of cellular C during recovery, was also still as high as $10.1 \text{ mol mol}^{-1}$. These ratios imply that not only did the formerly nitrogen-starved *Thalassiosira weissflogii* have slightly less N content per cell than they would have had if they had recovered from silicon starvation, they were also still quite deficient in N relative to other major nutrient elements.

It is worth pointing out that the cellular elemental quotas and ratios at the end of the recovery stages of the 2 experiments were attained in fundamentally different ways. The cells' recovery from silicon starvation entailed acquiring Si for the construction of the cell wall, while their recovery from nitrogen limitation required bringing themselves back from a physiological extreme (C/N ratios $> 20 \text{ mol mol}^{-1}$, C/P ratios $> 130 \text{ mol mol}^{-1}$ and N/P ratios $< 6 \text{ mol mol}^{-1}$). In the NSE, cellular quotas of N and P increased during the RS because nutrients were being taken up but the cells were not dividing. In the SSE, the amount of N and P per cell decreased during the RS due to the suddenly high rates of cell division after DSi readdition (Fig. 1). The decline in cellular C during the recovery from nitrogen starvation was due to the net consumption of cellular energy stores, while the decline in C per cell during the recovery from silicon starvation was due to the rapid cell division that was occurring (Fig. 1f).

Shifts in elemental composition during the experiment

The episodes of growth through to nutrient exhaustion, nutrient starvation, nutrient resupply and 24 h of recovery in both the NSE and the SSE resulted in cells at the end of the experiment containing markedly lower amounts of N and P but relatively similar amounts of Si and C compared with cells at the beginning of the experiment (Fig. 4). By the end of the experiments, cellular P content had declined from ~ 0.3 to $0.09 \text{ pmol cell}^{-1}$, a decrease of 70%. The net decline in N per cell was 70% in the NSE and 51% in the SSE. But even at the end of the SSE, Si per cell was only 9% lower than at the beginning of the experiment (and by the end of the NSE, it had actually increased by 6%).

The observed decrease in N and P quotas in both the NSE and SSE contradicts the idea that the Si-starved cells would continue to take up nitrate and phosphorus during Si starvation, causing an increase in cellular stores of N and P. The overall lowering of N and P quotas, while perhaps related to the overall decline in nitrate and phosphate concentrations, may indicate a decline in the overall health of cells exposed to 24 h of

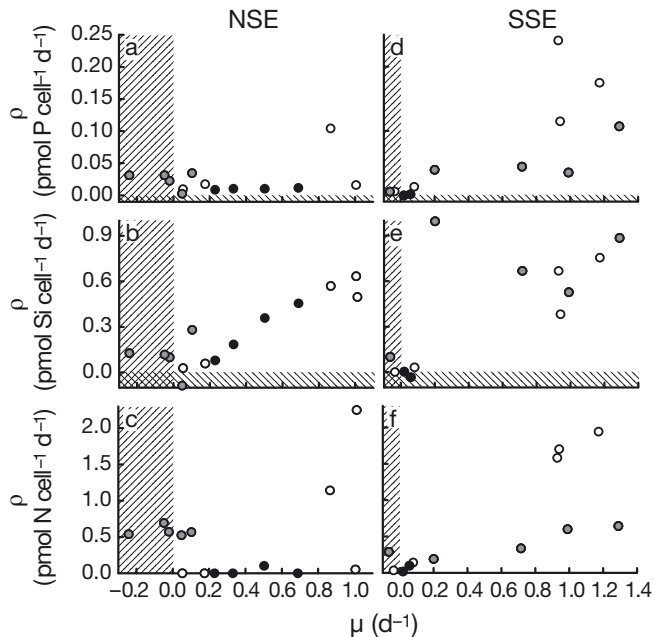


Fig. 8. *Thalassiosira weissflogii*. Cell-specific rates of net phosphate, DSi and nitrate uptake versus the concentration of the limiting nutrient in the (a–c) NSE and (d–f) SSE. Hatched areas contain values below 0. (○) IGS and 1st Starvation Stage, (○) Recovery Stage, (●) 2nd Starvation Stage. In each of panels (a) and (d), 1 point with a value greater than $2.5 \text{ pmol cell}^{-1} \text{ d}^{-1}$ has been omitted

nutrient starvation, be it N starvation or Si starvation. This is supported by the fact that after nutrient starvation, net cell-specific rates of nitrate uptake and phosphate uptake were lower, both with respect to growth rate and in general, than they were during the IGS of the experiments (Fig. 8).

Not only was the amount of Si per cell similar between the beginning and end of the experiments, the overall variation in Si per cell was also relatively minor. The highest value of $0.73 \pm 0.01 \text{ pmol Si cell}^{-1}$ was only 40% larger than the lowest value of $0.53 \pm 0.07 \text{ pmol Si cell}^{-1}$, and the lowest value was only 20% below the overall average of $0.66 \pm 0.05 \text{ pmol Si cell}^{-1}$ (Fig. 4b,f). The highest value of N per cell was, in contrast, 4 times the lowest value, and the highest value of P per cell was 3 times the lowest value. This is related to the fact that the half of the frustule handed down to each daughter cell cannot be remodeled, which puts serious limits on the changes in cellular silicon quotas that are possible over just a few generations.

Patterns of uptake of the nonlimiting nutrients

In the experiments, net cell-specific rates of nutrient uptake were overwhelmingly highest during the IGS (Fig. 3). As this occurred after several weeks of unin-

terrupted exponential growth under high nutrient conditions, the high net rates of nutrient acquisition may have related to a surfeit of transport systems, cellular resources and energy that did not reoccur during the experiment. The high rates could not even be supported to the end of the IGS (throughout which exponential cell growth occurred). Cell-specific rates of nutrient uptake, not only for nitrate in the NSE and DSi in the SSE, but for phosphate in both experiments, decreased during the IGS in relation to the decline in the limiting nutrient (Figs. 3 & 7).

The notable drop in cell-specific rates of uptake of the nonlimiting nutrient, phosphate, during the IGS of both experiments occurred alongside a notable decline in P content per cell (Fig. 4a,e). Phosphate concentrations were relatively high ($>9 \mu\text{M}$) and the ratio of nitrate to phosphate in the media was low ($<3 \text{ mol mol}^{-1}$), so the declines in phosphate uptake and P per cell were not driven by declining phosphate availability. The decline in the cellular phosphate stockpile must have been related instead to diminished cellular resources (including energy) as nitrate became increasingly less available. This would, in turn, suggest that the storage of 'luxury' P occurs only when there is an excess of available P and cells have the energy and resources for taking it up and storing it.

Although the cellular P quotas showed fairly straightforward behaviour with each stage of the experiments (Fig. 4a,e), there was no single factor controlling the changes in net cell-specific rates of phosphate uptake. These did not scale to the growth rate (Fig. 8a,d, Tables 2 & 3), they bore no relationship to phosphate concentrations (not shown) and they were only related to concentrations of the limiting nutrient during the IGS (Fig. 7a,b). In both experiments phosphate uptake seemed more to be tracking the general physiological condition of the cells. In the NSE, they declined with the limiting nutrient during the IGS, reached low values during the 1st NSS, recovered slightly during the RS and then dropped back down during the 2nd NSS. Phosphate uptake rates did much the same in the SSE, although in the RS of the SSE, net cell-specific rates of uptake were higher and more strongly related to growth rates than in the RS of the NSE (Figs. 7a,d & 8a,d).

In stark contrast to this, net cell-specific rates of DSi uptake in the NSE corresponded remarkably well with growth rates (Fig. 8b), especially during the IGS, 1st NSS and 2nd NSS. Given how well the 2nd NSS points (in black on Fig. 8b) align with the trend, it is tempting to conclude that when the cells were growing on internal stores of nitrogen, DSi acquisition was the rate-limiting step for cell division.

Cell-specific rates of nitrate uptake in the SSE were also strongly related to cellular growth rates (Fig. 8f)

rather than to concentrations of the limiting nutrient, DSi (Fig. 7f). Unlike the case for DSi in the NSE (Fig. 8b), however, in this case, there is a steeper relationship between the net cell-specific rate of nitrate uptake and growth rate during the IGS than during the RS (Fig. 8f). This would imply that although the silicon-starved cells quickly reattained maximal growth rates following DSi readdition, they did not fully recover their maximal physiological capabilities. This view is also supported by a similar pattern in the phosphate uptake data of the SSE (Fig. 8d).

Also, the uptake of both phosphate and nitrate effectively ceased when DSi concentrations became limiting. As noted above, Si-starved cells were not taking advantage of the time in terms of stockpiling the other nutrients.

Is silicon limitation better than nitrate limitation?

One of the questions that motivated this work is whether silicon limitation is advantageous to diatoms. This is a difficult question to answer and, as explained below, the data presented here do not resolve the issue. But it is worth considering the adaptiveness of the diatoms' response to silicon starvation versus their response to nitrogen starvation.

As has been shown here and in previous studies, nitrogen-starved cells are severely depleted in N (Fig. 4c) and, as a consequence of having related deficiencies in enzymes and proteins (Harrison et al. 1976, 1977, Sakshaug & Holm-Hansen 1977, Dortch 1982), must undergo 30 h of recovery after nutrients are resupplied before they are able to divide again (Fig. 1). Silicon-starved cells, however, just lack enough silicon to make 2 complete hypothecae and, thus, are able to divide again almost immediately following the resupply of DSi. The quicker recovery of silicon-starved cells could, in principle, help them to dominate in upwelling environments, where nutrients are delivered to the euphotic zone in pulses. Modelling has suggested, for example, that if an equal number of silicon-starved and nitrogen-starved cells competed for a new set of nutrients, the silicon-starved population would end up with the vast majority of the new nutrients because of its earlier resumption of cell division (De La Rocha & Passow 2004).

Whether this 'advantage in principle' translates into an 'advantage in reality' is difficult to ascertain. Unfortunately, in terms of the present experiment, the concentrations of the re-added nutrients became limiting again too soon for a proper comparison of the longer term consequences of nutrient starvation to be made. And in the natural environment, any possible advantage to an earlier resumption of growth upon nutrient

resupply could disappear with the increased number of cell divisions that are possible under nitrogen starvation or even with something as simple as differences in maximum possible photosynthetic rates between species or with differences in maximum possible growth rates of cells in the competing populations. The loss of cells during silicon starvation also indicates that these cells may be more open to infection or attack and their recovery from nutrient starvation in nature could be handicapped by this vulnerability.

The idea that the response to silicon starvation is adaptive compared with the response to nitrogen starvation depends on these 2 responses actually being different. Although the outcomes are different, and the behaviour of *Thalassiosira weissflogii* under silicon starvation appears different from its behaviour under nitrogen starvation, in a sense it is the exact same response to a lack of nutrients. In both cases the cells are growing for as long as supplies of the limiting nutrient are sufficient for a cell to produce 2 daughter cells. During nitrogen starvation, cellular nitrogen stores are divided up among increasingly N-poor daughter cells; growth ceases when absolutely minimum cellular quotas of N are reached. Under silicon starvation, because silica cannot be extracted from the silica valve that is passed down to a daughter cell, as soon as a cell cannot take up enough silicon to form a new hypotheca for each of the daughter cells, cell division ceases.

Thus, while silicon-starved diatoms in theory could still help diatoms to respond more quickly to upwelled nutrients than other co-occurring nitrogen-deficient phytoplankton, the physiological reaction to lack of DSi (immediate cessation of division) is more an accident of physiology (the immutability of the silica frustule) than an innovation for dealing with intermittent bouts of nutrient limitation.

LITERATURE CITED

- Blank GS, Robinson DH, Sullivan CW (1986) Diatom mineralization of silicic acid. VIII. Metabolic requirements and the timing of protein synthesis. *J Phycol* 22:382–389
- Brzezinski MA (1985) The Si:C:N ratio of marine diatoms: interspecific variability and the effect of some environmental variables. *J Phycol* 21:347–357
- Brzezinski MA (1992) Cell-cycle effects on the kinetics of silicic acid uptake and resource competition among diatoms. *J Plankton Res* 14:1511–1539
- Brzezinski MA, Olson RJ, Chisholm SW (1990) Silicon availability and cell-cycle progression in marine diatoms. *Mar Ecol Prog Ser* 67:83–96
- Collos Y (1980) Transient situations in nitrate assimilation by marine diatoms. 1. Changes in uptake parameters during nitrogen starvation. *Limnol Oceanogr* 25:1075–1081
- Coombs J, Darley WM, Holm-Hansen O, Volcani BE (1967) Studies on the biogeochemistry and fine structure of silica shell formation in diatoms. Chemical composition of *Nav-*

- icula pelliculosa* during silicon-starvation synchrony. Plant Physiol 42:1601–1606
- De La Rocha CL (2007) The biological pump. In: Elderfield H (ed) The oceans and marine geochemistry, Vol. 6. Holland HD, Turekian K (eds) Treatise on geochemistry, Update 1. Elsevier Pergamon, Oxford, p 1–29
- De La Rocha CL, Passow U (2004) Recovery of *Thalassiosira weissflogii* from nitrogen and silicon starvation. Limnol Oceanogr 49:245–255
- Dortch Q (1982) Effect of growth conditions on accumulation on internal nitrate, ammonium, amino acids and protein in three marine diatoms. J Exp Mar Biol Ecol 61:243–264
- Dortch Q, Clayton JR Jr, Thoresen SS, Ahmed SI (1984) Species differences in accumulation of nitrogen pools in phytoplankton. Mar Biol 81:237–250
- Dugdale RC, Wilkerson FP, Minas HJ (1995) The role of a silicate pump in driving new production. Deep-Sea Res I 42: 697–719
- Flynn KJ, Martin-Jézéquel V (2000) Modelling Si-N limited growth of diatoms. J Plankton Res 22:447–472
- Flynn KJ, Davidson K, Leftly JW (1994) Carbon-nitrogen relations at whole-cell and free-amino-acid levels during batch growth of *Isochrysis galbana* (Prymnesiophyceae) under conditions of alternating light and dark. Mar Biol 118:229–237
- Geider RJ, La Roche J (2002) Redfield revisited: variability of C:N:P in marine microalgae and its biochemical basis. Eur J Phycol 37:1–17
- Guillard RRL (1975) Culture of marine phytoplankton for feeding marine invertebrates. In: Smith WL, Chanley MH (eds) Culture of marine invertebrate animals. Plenum Press, New York, p 26–60
- Harrison PJ, Conway HL, Dugdale RC (1976) Marine diatoms grown in chemostats under silicate or ammonium limitation. I. Cellular chemical composition and steady-state growth kinetics of *Skeletonema costatum*. Mar Biol 35: 177–186
- Harrison PJ, Conway HL, Holmes RW, Davis CO (1977) Marine diatoms grown in chemostats under silicate or ammonium limitation. III. Cellular chemical composition and morphology of *Chaetoceros debilis*, *Skeletonema costatum*, and *Thalassiosira gravida*. Mar Biol 43:19–31
- Harrison PJ, Thompson PA, Calderwood GS (1990) Effects of nutrient and light limitation on the biochemical composition of phytoplankton. J Appl Phycol 2:45–56
- Laws EA, Bannister TT (1980) Nutrient- and light-limited growth of *Thalassiosira fluviatilis* in continuous culture, with implications for phytoplankton growth in the ocean. Limnol Oceanogr 25:457–473
- Martin-Jézéquel V, Hildebrand M, Brzezinski MA (2000) Silicon metabolism in diatoms: implications for growth. J Phycol 36:821–840
- Olson RJ, Vault D, Chisholm SW (1986) Effects of environmental stresses on the cell cycle of two marine phytoplankton species. Plant Physiol 80:918–925
- Sakshaug E, Holm-Hansen O (1977) Chemical composition of *Skeletonema costatum* (Grev.) Cleve and *Pavlova (monochrysis) lutheri* (Droop) as a function of nitrate-, phosphate-, and iron-limited growth. J Exp Mar Biol Ecol 29:1–34
- Schlitzer R (2000) Electronic atlas of WOCE hydrographic and tracer data now available. Eos Trans AGU 81:45
- Smetacek VS (1985) Role of sinking in diatom life-history cycles: ecological, evolutionary, and geological significance. Mar Biol 84:239–251
- Strickland JDH, Parsons TR (1972) A practical handbook of seawater analysis, 2nd edn. Fish Res Board Can Bull 167
- Vault D, Olson RJ, Merke S, Chisholm SW (1987) Cell-cycle response to nutrient starvation in two phytoplankton species, *Thalassiosira weissflogii* and *Hymenomonas carterae*. Mar Biol 95:625–630

Appendix 1. Results from the nitrogen and silicon starvation experiments (NSE and SSE, respectively)

Table A1. *Thalassiosira weissflogii*. Directly measured values from the NSE. Values represent the average \pm SD of samples from 2 replicate incubation bottles

Time (h)	DSi (μ M)	Phosphate (μ M)	Nitrate (μ M)	No. cells ml ⁻¹ ($\times 10^4$)	C cell ⁻¹ (pmol)	N cell ⁻¹ (pmol)	Si cell ⁻¹ (pmol)
0	104	12.9	35	0.015	13.3	2.47	0.68
95	101 \pm 3	10.5 \pm 0.4	17 \pm 1	0.84 \pm 0.02	14.6 \pm 0.3	2.95 \pm 0.04	0.64 \pm 0.02
119	93 \pm 5	9.1 \pm 0.0	2 \pm 2	2.00 \pm 0.25	11.0 \pm 0.3	2.03 \pm 0.13	0.66 \pm 0.01
143	71 \pm 1	8.5 \pm 0.2	0 \pm 0	5.46 \pm 0.01	9.8 \pm 0.2	0.81 \pm 0.00	0.62 \pm 0.02
167	68 \pm 4	7.5 \pm 0.0	0 \pm 0	6.51 \pm 0.11	10.8 \pm 0.2	0.66 \pm 0.02	0.63 \pm 0.01
236	62 \pm 4	5.6 \pm 0.1	0 \pm 0	7.47 \pm 0.02	12.7 \pm 0.1	0.57 \pm 0.01	0.61 \pm 0.04
237	60 \pm 3	5.3 \pm 0.1	46 \pm 1	7.33 \pm 0.44	13.0 \pm 0.8	0.58 \pm 0.05	0.65 \pm 0.06
239	61 \pm 2	5.3 \pm 0.2	42 \pm 0	7.43 \pm 0.07	12.5 \pm 0.1	0.62 \pm 0.01	0.63 \pm 0.01
242	60 \pm 2	5.0 \pm 0.3	37	7.50 \pm 0.00	12.7 \pm 0.0	0.68 \pm 0.01	0.64 \pm 0.00
246	56 \pm 0.3	4.6 \pm 0.0	30	7.36 \pm 0.17	11.3 \pm 0.1	0.69 \pm 0.00	0.66 \pm 0.02
252	55 \pm 1	4.2 \pm 0.1	21 \pm 0	7.33 \pm 0.42	11.1 \pm 0.5	0.80 \pm 0.04	0.66 \pm 0.03
261	51 \pm 0	3.4 \pm 0.1	2 \pm 1	7.20 \pm 0.15	12.1 \pm 0.4	1.20 \pm 0.04	0.72 \pm 0.04
267	45 \pm 1	3.2 \pm 0.0	0 \pm 0	8.17 \pm 0.27	11.9 \pm 0.2	1.10 \pm 0.02	0.73 \pm 0.00
271	38 \pm 1	3.0 \pm 0.0	0 \pm 0	9.16 \pm 0.44	9.7 \pm 0.9	0.86 \pm 0.06	0.73 \pm 0.04
285	27 \pm 1	2.4 \pm 0.1	0 \pm 0	11.18 \pm 0.45	10.5 \pm 0.5	0.83 \pm 0.01	0.72 \pm 0.04
291	25 \pm 1	2.2 \pm 0.0	0 \pm 0	11.84 \pm 0.18	11.4 \pm 0.3	0.76 \pm 0.02	0.70 \pm 0.01

Table A2. *Thalassiosira weissflogii*. Directly measured values from the SSE. Values represent the average \pm SD of samples from 2 replicate incubation bottles

Time (h)	DSi (μM)	Phosphate (μM)	Nitrate (μM)	No. cells ml^{-1} ($\times 10^4$)	C cell $^{-1}$ (pmol)	N cell $^{-1}$ (pmol)	Si cell $^{-1}$ (pmol)
0	29	12.8	259	0.015	15.6	2.85	0.68
98	24 \pm 0	11.1 \pm 0.2	248 \pm 1	0.63 \pm 0.02	–	–	0.66 \pm 0.03
121	15 \pm 3	9.1 \pm 0.5	226 \pm 9	2.00 \pm 0.53	14.0 \pm 1.3	2.54 \pm 0.23	0.63 \pm 0.02
145	3 \pm 1	5.3 \pm 1.0	170 \pm 13	5.11 \pm 0.27	13.4 \pm 1.1	2.19 \pm 0.05	0.53 \pm 0.07
169	1 \pm 2	4.7 \pm 0.1	163 \pm 0	5.54 \pm 0.09	15.9 \pm 0.5	2.10 \pm 0.06	0.54 \pm 0.01
238	5 \pm 6	3.8 \pm 0.3	158 \pm 1	5.00 \pm 0.13	20.0 \pm 1.2	2.28 \pm 0.13	0.63 \pm 0.01
239	53 \pm 6	3.9 \pm 0.3	158 \pm 0	5.05 \pm 0.04	20.7 \pm 0.2	2.29 \pm 0.02	0.68 \pm 0.02
242	47 \pm 1	3.7 \pm 0.2	157 \pm 0	5.18 \pm 0.02	20.3 \pm 0.1	2.29 \pm 0.02	0.70 \pm 0.03
245	41 \pm 1	2.9 \pm 0.1	152 \pm 0	6.08 \pm 0.07	17.7 \pm 0.3	2.00 \pm 0.03	0.67 \pm 0.01
248	35 \pm 3	2.6 \pm 0.1	150 \pm 0	6.65 \pm 0.03	17.0 \pm 0.2	1.88 \pm 0.00	0.73 \pm 0.01
263	3 \pm 2	0.5 \pm 0.1	113 \pm 6	12.35 \pm 0.06	10.6 \pm 0.8	1.40 \pm 0.15	0.67 \pm 0.03
269	4 \pm 3	0.5 \pm 0.1	109 \pm 7	12.16 \pm 0.18	11.0 \pm 0.8	1.33 \pm 0.10	0.65 \pm 0.01
287	5 \pm 6	0.3 \pm 0.0	98 \pm 3	12.69 \pm 0.62	11.3 \pm 0.6	1.34 \pm 0.08	0.64 \pm 0.03
311	5 \pm 4	0.4 \pm 0.1	96 \pm 3	12.94 \pm 0.16	12.2 \pm 0.3	1.40 \pm 0.05	0.62 \pm 0.01

Editorial responsibility: Graham Savidge,
Portaferry, UK

Submitted: February 12, 2010; Accepted: June 10, 2010
Proofs received from author(s): August 8, 2010